Synthesis of Silica Coating Derived from Geothermal Solid Waste Modified with 3-Aminopropyl Triethoxysilane (APTES) and Silver Nano Particles (AgNPs)

S. Silviana
Department of Chemical Engineering, Faculty of Engineering, Diponegoro University

Angga Gata Hasega
Department of Chemical Engineering, Faculty of Engineering, Diponegoro University

Aulia Rizqy Nur Hanifah
Department of Chemical Engineering, Faculty of Engineering, Diponegoro University

Afriza Ni' matus Sa' adah
Department of Chemical Engineering, Faculty of Engineering, Diponegoro University

https://doi.org/10.5109/6625733

出版情報：Evergreen. 9 (4), pp.1224-1230, 2022-12. 九州大学グリーンテクノロジー研究教育センター
バージョン：

Synthesis of Silica Coating Derived from Geothermal Solid Waste Modified with 3-Aminopropyl Triethoxysilane (APTES) and Silver Nano Particles (AgNPs)

S. Silviana*, Angga Gata Hasega, Aulia Rizqy Nur Hanifah, Afriza Ni'matus Sa'adah

Department of Chemical Engineering, Faculty of Engineering, Diponegoro University
Jl. Prof. Soedarto, SH, UNDIP Tembalang Campus, Semarang, Indonesia 50275

*Author to whom correspondence should be addressed:
E-mail: silviana@che.undip.ac.id

(Received February 11, 2022; Revised December 16, 2022; accepted December 25, 2022).

Abstract: The hydrophobic and antibacterial coatings derived from geothermal waste silica modified by APTES and AgNPs. The paper aims are to investigate contact angle (CA) and antibacterial test from the coating upon ethanol, sodium silicate, water, and APTES; to characterize silica raw by XRD, and coating product by SEM EDX. The research was conducted by sodium silicate preparation, AgNPs synthesis, silica-APTES on the glass, and AgNPs layer on the coated glass. The result showed that the CA attained in range of 20-50° with bacterial inhibition diameter of 10 mm and 12 mm for *E.coli* and *S. aureus*, respectively.

Keywords: APTES; AgNPs; coating; sodium silicate; geothermal

1. Introduction

Water is the primary factor that causes iron rusting and weathering of material. Therefore, efforts are needed to extend the material's shelf life because it also acts as a medium for the growth of bacteria when damaged. According to research, bacteria can adapt and survive in acidic environments (low pH) and under osmotic pressure. In addition to extending the shelf life of a material, efforts to protect it from bacteria are also needed.

The process of hydrophobic surfaces coating has attracted much attention due to its ability to self-clean, anti-ice, separate water, and oil reduce surface spillage, etc[1]. Although this method is able to reduce the adhesion of bacteria, it is unable to sterilize the material, thereby making it wet after being exposed to a humid environment for a long time. The hydrophobic surface also tends to lose its hydrophobicity after the presence of a biofilm layer formed by bacteria[2]. Therefore, one of the methods used to overcome these problems is the application of hydrophobic and antibacterial coatings.

The manufacture of hydrophobic and antibacterial coatings requires several materials such as precursors, modifying, and antibacterial agents. Commonly used precursors are tetraethoxysilane (TEOS), sodium silicate, and methyltrimethoxysilane (MTMS). Previous researchers developed silica coatings from diethoxydimethylsilane (DEODMS), methyltriethoxysilane (MTEOS), and tetraethoxysilane (TEOS)[3]. However, the use of DEODMS, MTEOS, and TEOS are ineffective in large-scale industries because they are expensive, difficult to obtain, and possess toxic properties.

Silica has the molecular formula SiO_2 (silicon dioxide), obtained from mineral, crystalline silica, and waste[4,5]. It is an inert substance with good adsorption properties, excellent ion exchange, and easily adjustable with certain chemical compounds[6]. Silica can be used as a catalyst, adsorbent[7–12], filter media[13], desiccant materials[14,15], thermal purification material[16], and coating material[17]. Research on silica sources, such as fly ash[18], bamboo leaves[19], bagasse solid waste[20], and geothermal solid waste have been widely conducted[21,22].

This research used the geothermal solid waste from PT Geo Dipa Energi as a silica source due to the high silica oxide content of up to 88.29%[23]. The process of transforming geothermal energy into electricity leads to the production of solid brine waste in the form of slurry. The remaining contents of the geothermal solid waste consist of several inorganic materials in trash composition, such as arsenic, barium, boron, cadmium, chromium, copper, lead, mercury, selenium, silver, and zinc[24]. The selection of geothermal solid waste as a source of silica is very appropriate due to its geothermal abundance potential of approximately 28 GW[25–27].

The selection of a modifying agent is closely related to the type of antibacterial material used. The material used was coated per layer against bacterial using tannin-Fe^{3+}

and polyethyleneimine[28]. The results obtained that the coating (TA-Fe^{3+}/PEI) has effective antibacterial properties on the contact layer. However, the use of tannins and Fe^{3+} is not stable in practical applications. The AgNPs have chemical stability, therefore, they can be used as an antibacterial agent[29]. The use of silica-AgNPs coating with various types of modifying agents, such as (3-Aminopropyl) triethoxysilane (APTES), N-[3-(trimethoxysilyl)propyl] ethylenediamine (AEPTMS), (3-Mercaptopropyl) trimetoxysilane (MPTMS) have been conducted previously[30]. The best results were obtained with the use of the APTES modifying agent. In this research, silica derived from geothermal solid waste was modified with APTES and AgNPs, which were used as modifying and antibacterial agents.

This research aims to obtain the best composition of hydrophobic coatings at concentrations of sodium silicate, ethanol, water, and APTES. It also used a graphical contact angle response to obtain the best composition of antibacterial coatings in the variable range of $AgNO_3$ concentrations coated with Si-APTES with the response of the inhibition of gram-positive (*S. aureus*) and gram-negative (*E. coli*) bacteria. Furthermore, the process was used to characterize the coating on the coated glass with SEM-EDX and XRD.

2. Materials and Methods

The materials used in this research were geothermal solid waste from PT Geo Dipa Energi, (3-Aminopropyl) triethoxysilane (APTES) 98% MERCK, Ammonia solution 25% MERCK, ethanol 99.9% MERCK, NaOH, $AgNO_3$ MERCK, Aquadest, Poly sodium 4-styrenesulfonate (PSSS), Ascorbic acid, $NaBH_4$, and Trisodium citrate Sigma Aldrich.

The silica from geothermal solid waste was prepared in accordance with preliminary research[23]. Silica from PT Geo Dipa Energi was dried using the oven to remove the water content and pounded on a mortar to reduce its size. The obtained content was analyzed by X-Ray Fluorescence Spectrometry (XRF).

Purification of silica from geothermal solid waste was carried out in accordance with previous research[31]. Inorganic impurities from geothermal solid waste were removed by mixing 20% sulfuric acid solution with 10 grams dried silica (ratio 1:4 w/v) by heating for 105 minutes at 100 °C under constant stirring. Before drying, the solid was washed until the filtrate became neutral. The dried silica was analyzed by X-Ray Fluorescence Spectrometry (XRF) to determine the concentration of silica and its impurities (Fe and Al).

Synthesis of sodium silicate in this research was carried out with some modifications[32]. Several variations of sodium silicate were made by mixing the purified silica with 200 ml of 2 N NaOH. The mixture was heated and stirred at a constant speed using a magnetic stirrer at 90 ^oC. After the solution was cooled, it was filtered to obtain a filtrate in the form of sodium silicate solution.

Synthesis of colloidal silica solution was conducted with some modifications[33]. Colloidal silica was made by hydrolysis and condensation using an alkaline catalyst. Furthermore, sodium silicate, ammonia, water, and ethanol were mixed with the composition according to the variable. The sol was aged at room temperature for 18 hours, and then filtered to remove the sediment.

Synthesis of silica-APTES layer on glass is in accordance with preliminary research with some of the modifications[33,34]. The spray coating method carried out the formation of a hydrophobic layer on the glass surface. Firstly, the material was cleaned by immersing it in 98% methanol followed by 98% acetone solution for 15 minutes. The samples were then dried in an oven and cooled in a desiccator[34]. The coating was prepared using the spray method, followed by the curing process at 80 °C for 2 minutes. It was further dried at room temperature for 24 hours[33].

AgNPs were synthesize based on previous research with some modifications[33]. It was prepared using a seed-mediated method which consisted of two steps: (1) producing a solution of silver nanoparticles and (2) growing AgNPs nanoprisms. Silver seeds were obtained by mixing trisodium citrate solution (20 mL, 25 mM), PSSS (1 mL, 0.5 g/L), and $NaBH_4$ (1.2 mL, 10 mM), followed by the addition of 20mL $AgNO_3$ solution at a varying rate of 2 mL/min.

AgNPs were prepared by mixing 35 ml of aquadest, ascorbic acid solution (0.525 mL, 10 mM), and 0.56 ml of the previously prepared silver seeds. This was followed by the addition of 21 mL $AgNO_3$ solution at varying concentrations of 1 mL/min.

Surface silanization and formation of AgNPs layer was conducted in accordance with previous research[33]. The glass substrate coated with a colloidal silica solution was functionalized with APTES after it was dissolved in varying n-hexane. After that, the coating on the glass substrate was formed by the spray coating method and dried at room temperature. For the formation of the AgNPs layer, the coated substrate glass was immersed in the previously prepared solution. The soaking process was left at room temperature for 24 hours, washed with distilled water, and dried.

3. Results and Discussion

In this research, the purification of geothermal solid waste was conducted by leaching using sulfuric acid. Figure 1 shows that the minerals in the geothermal solid waste are K, Ca, Cr, Mn, Fe, Cu, Zn, As, Br, Eu, Re, Pb, and Si, which has the largest percentage of 80.7%. XRF analysis results on geothermal solid waste before and after the leaching process showed a difference in the percentage of silica content.

In the acid leaching process, the solution can dissolve the metal, thereby reducing the composition of unimportant metal oxides. A decrease in metal oxide levels leads to an increase in SiO_2[18].

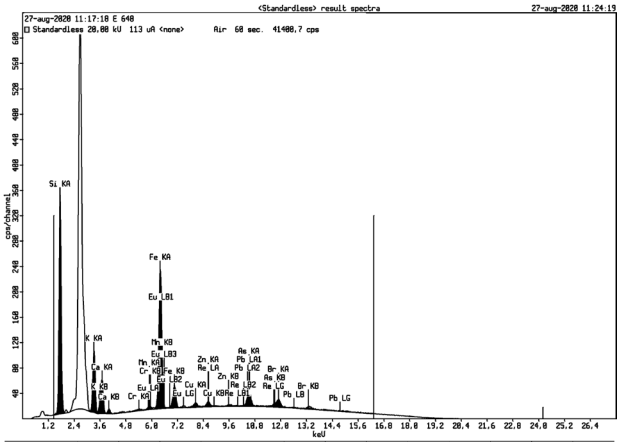

Compound	Si	K	Ca	Cr	Mn	Fe	Cu	Zn	As	Br	Eu	Re	Pb
Conc	80,7	8,37	3,63	0,079	0,07	4,82	0,15	0,14	0,69	0,57	0,3	0,2	0,3
Unit	%	%	%	%	%	%	%	%	%	%	%	%	%

Fig. 1: XRF analysis of geothermal solid waste before leaching process.

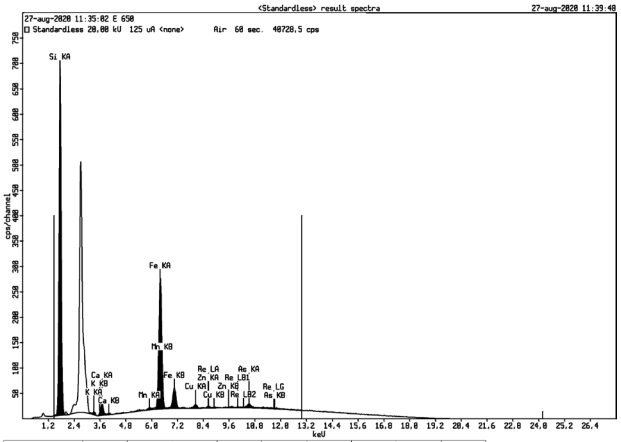

Compound	Si	K	Ca	Mn	Fe	Cu	Zn	As	Re
Conc	95,1	0,35	1,0	0,061	3,12	0,083	0,01	0,12	0,1
Unit	%	%	%	%	%	%	%	%	%

Fig. 2: XRF analysis of geothermal solid waste after the leaching process.

Furthermore, its color can change from gray to white after leaching treatment. The color change indicates that the metals have dissolved, and after the leaching process, it increases by 95.1%, according to the XRF analysis results shown in Fig. 2.

3.1 Effect of Ethanol Volume on Contact Angle

In this research, variations of ethanol volume were conducted to determine the effect of increasing the ethanol volume on contact angle. The test was performed to characterize the surface wettability of substrates using ethanol variations of 0.05 ml, 0.15 ml, 0.5 ml, 1 ml, and 2 ml[35]. Furthermore, silica, water, ammonia solution, and APTES are fixed variables. Fig. 3 shows that the addition of ethanol volume on the hydrophobic properties of the coating process fluctuates the contact angle.

The best results were obtained with the addition of 0.5 mL of ethanol at a contact angle of 49.83°. Meanwhile, the addition of 1 mL and 2 mL ethanol produced the lowest contact angles of 29.67° and 41.75°.

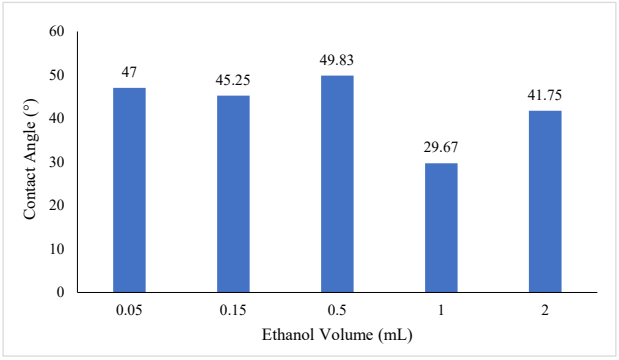

Fig. 3: XRF analysis of geothermal.

This research was carried out using undiluted ethanol. The contact angle obtained was greater when compared to previous research concerning the effect of the water-ethanol ratio on the hydrophobic surface. The use of pure ethanol (100%v) produced the lowest contact angles of 28° at high surface affinity[36]. The increase in ethanol ratio leads to a decrease in the contact angle obtained. Hydrophilic materials will support water spread and produce a low contact angle[37].

3.2 Effect of Silica Concentration on Contact Angle

The effect of precursors on hydrophobic properties was analyzed by varying the silica concentration started from 3, 4, 5, 6, and 7 %w/v. The composition solution of ammonia, ethanol, water, and APTES was determined as a fixed variable. Fig. 4 shows the increase in silica concentration on the hydrophobic properties of the coating decreases the contact angle.

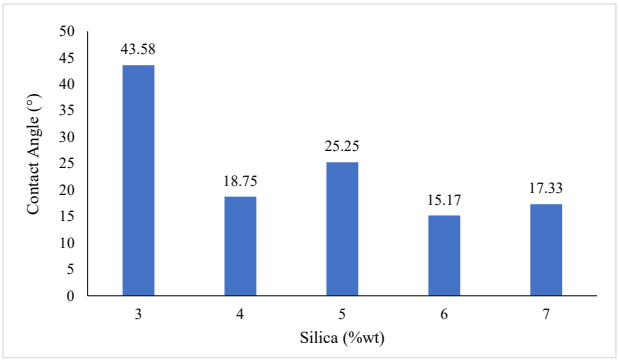

Fig. 4: Effect of silica concentration on the hydrophobic properties of the coating.

The best results were obtained at 3 %wt silica concentration at contact angle of 43.58°. These results are in accordance with previous researchers on the effect of silica concentration on contact angle[38]. This is due to the presence of OH functional group on the nanoparticles. Therefore, an increase in the silica concentration leads to a rise in the Si-OH functional group formed. The OH functional group on silica nanoparticles increases the hydrophilicity of the coating and reduces the value of the contact angle[39,40].

3.4 Effect of Water Volume on Contact Angle

The effect of water on hydrophobic properties was analyzed by varying the volume ranging from 1, 3, 5, 7, and 10 ml. The composition of the solution of ammonia, ethanol, silica, and APTES was determined as a fixed variable. Fig. 5 shows that the increase in water volume on the hydrophobic properties of the coating process leads to a rise in the contact angle obtained.

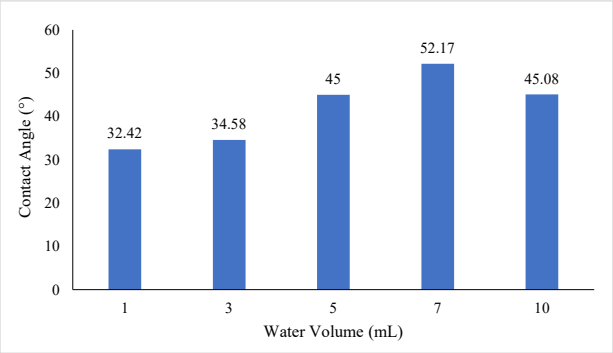

Fig. 5: Effect of water volume on the hydrophobic properties of the coating.

The use of 7 mL water volume produces a contact angle of 52.17°. However, the use of 10 mL water volume led to a contact angle of 45.08°. These results are in accordance with previous researchers concerning the effect of the ratio of water to glass with TEOS as a modifying agent[41]. The resulting contact angle increased and also decreased to 143.86±0.43° and 141.70±0.63°, respectively.

The water volume can affect the colloidal properties of the mixture, which are the main factor in the formation of nano-sized particles. The decrease in particle size increases the surface hydrophobicity formed because the silica surface was modified by the exchange of a hydroxyl group (-OH) with an amine group (-NH_2) from APTES. Furthermore, the increase in water volume leads to a rise in surface modification of silica by the amine group, thereby increasing the surface hydrophobicity. The decrease in contact angle is due to the presence of a large water fraction, which makes the surface less evenly distributed. The non-hydrophobic surface is caused by the presence of gaps filled by water which easily interacts with ethanol molecules. This causes the hydrophobic structure of silica to be weak. When the silica pores containing ethanol are dried, the ethanol evaporates along with Si-NH_2, thereby reducing surface hydrophobicity[41].

3.5 Effect of APTES Concentration on Contact Angle

The APTES concentration as a variable can affect the hydrophobic properties at variations of concentrated n-hexane (solvent) starting from 1, 2, 3, 4, and 5 %v/v. The composition of the solution of ammonia, ethanol, Na_2SiO_3, and water was used as fixed variables. The effect of APTES concentration on the hydrophobic properties of the coating process is shown in Fig. 6.

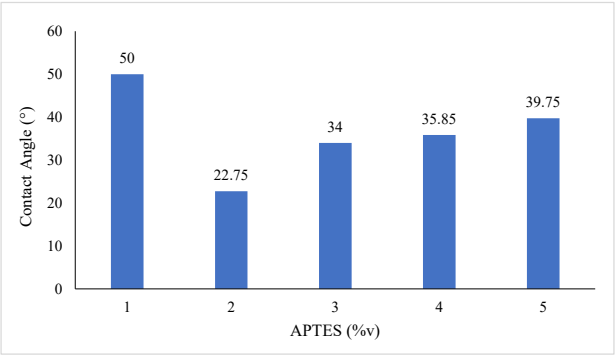

Fig.6: Effect of APTES concentration on the hydrophobic properties of the coating.

The highest (50°) and lowest (22.75°) contact angles of APTES were obtained at 1%v and 2 %v. These results can be explained by Kim and Kwon (2017)[42] on the effect of variations in APTES concentration with a contact angle of 40.6° and 74.2° at 1% and 17%v, respectively.

The polarity, porosity, and roughness are used to denote the surface properties of the contact angle. Surface modification of silica with APTES fails to produce high hydrophobic properties due to the non-polar amine group. However, the amine group increases the surface roughness and hydrophobicity. Therefore, the increasing contact angle can be caused by a rise in surface roughness[33].

According to previous research, there are three processes for the formation of APTES at various concentrations[42]. The process of salinization with the variation of APTES concentration in the solvent is shown in Fig. 6. The low concentration of APTES leads to prolonged diffusion time of the silane molecule to the silica surface. This indicates it can be polymerized in the solvent before reacting with the OH groups on the surface. These polymerized molecules create local nucleation, and diffusion accelerates agglomeration. Conversely, the high concentration of APTES leads to a faster reaction between the silane and the surface OH groups than the polymerization process. This leads to a more uniform surface of the silane than the lower APTES concentrations. A rise in the silane concentration further increases the molecule's spread to the surface. However, increasing the silane concentration does not guarantee surface alignment. This results in randomly oriented silane polymerization and eventually forms a rough surface.

3.6 Effect of $AgNO_3$ on Antibacterial Properties

The effect of $AgNO_3$ on antibacterial properties was analyzed by varying the concentration from 0.5 mM, 1 mM, 2.5 mM, 5 mM, and 10 mM. Antibacterial properties can be determined by performing disc diffusion analysis using gram-positive *(Staphylococcus aureus)* and gram-negative *(E. coli)* bacteria. Gram-positive bacteria have a single membrane covered with thick peptidoglycan. Meanwhile, gram-negative bacteria have a cell wall consisting of a layer of endotoxin lipopolysaccharide.

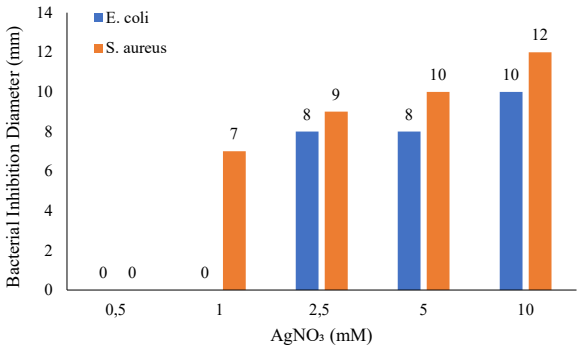

Fig.7: Effect of $AgNO_3$ concentration on the inhibition of bacteria

Fig. 7 shows that the concentration of $AgNO_3$ was directly proportional to the inhibitory power of the bacteria. The optimum condition of bacterial inhibition was obtained at $AgNO_3$ of 10 mM with an inhibitory diameter of 10 mm (*E. coli*) and 12 mm (*S. aureus*). The results obtained have greater bacterial inhibition compared to preliminary research. Previous result from other researchers investigated the effect of $AgNO_3$ concentration on the inhibition of gram-negative bacteria (*E. coli*) with an inhibitory diameter of 4.92 mm - 8.95 mm[43]. Meanwhile, previous researchers analyzed the effect of $AgNO_3$ concentration on the inhibition of gram-positive bacteria (*S. aureus*) at diameters of 2-6 mm[44]. In the manufacture of antibacterial materials, silver (Ag) acts as a strong antibacterial agent to the material[45].

3.7 SEM-EDX Analysis

The coating solution was characterized by Scanning Electron Microscope-Energy Dispersive X-Ray (SEM-EDX) analysis to determine the silica's surface morphology[46]. The goal of EDX characterization is to determine the difference in composition obtained.

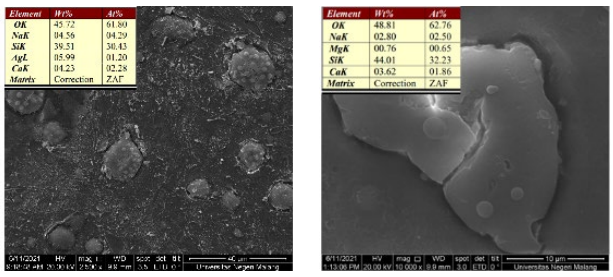

Fig.8: The SEM EDX Mapping results (a) 10 mM AgNPs (b) 0.5 mM AgNPs.

Figs. 8 (a) and (b) show SEM-EDX Mapping results used to visualize the morphology and mapping on a coated material. The result showed varying components between 10 mM AgNPs and 0.5 mM AgNPs. The coating solution with 0.5 mM AgNPs had a higher Si percentage than those with 10 mM AgNPs.

4. Conclusion

In conclusion, the composition of hydrophobic properties was obtained at 3 mL ammonia, 0.5 mL ethanol, 3% wt silica concentration, 7 ml water volume, and 1%v APTES. The composition of antibacterial properties was obtained at $AgNO_3$ 10 mM. Furthermore, based on SEM-EDX analysis, the largest silica percentage was found at a concentration of 0.5 mM AgNPs.

Acknowledgements

The authors would like to acknowledge the Advanced Material Laboratory (AMaL), Diponegoro University, Indonesia for all support and discussion during the research.

References

1) S. Xu, Q. Wang, N. Wang, and X. Zheng, "Fabrication of superhydrophobic green surfaces with good self-cleaning, chemical stability and anti-corrosion properties," *J. Mater. Sci.*, **54** (*19*) 13006–13016 (2019). doi:10.1007/s10853-019-03789-x.
2) F.Q. Dong, G.W. Li, Z.G. Sun, G. Shen, Q.M. Feng, and Q.W. Dai, "Preparation and antimicrobial ability of natural porous antibacterial materials," *J. Cent. South Univ. Technol. (English Ed.*, **12** (*4*) 370–375 (2005). doi:10.1007/s11771-005-0163-1.
3) M. Quinet, B. Neveu, V. Moutarlier, P. Audebert, L. Ricq, "Corrosion protection of sol–gel coatings doped with an organic corrosion inhibitor: Chloranil," *Prog. Org. Coat.*, **58** 46-53 (2007). doi: :10.1016/ j.porgcoat. 2006.11.007
4) V.P. Della, I. Kühn, and D. Hotza, "Rice husk ash as an alternate source for active silica production," *Mater. Lett.*, **57** (*4*) 818–821 (2002). doi:10.1016/ S0167-577X(02)00879-0.
5) M.R.F. Gonçalves, and C.P. Bergmann, "Thermal insulators made with rice husk ashes: production and correlation between properties and microstructure," *Constr. Build. Mater.*, **21** (*12*) 2059–2065 (2007). doi:10.1016/j.conbuildmat.2006.05.057.
6) X. Wanga, Z. Yea, Lifeng Chenb, Q. Zhenga, C. Liua, S. Ninga, A. Khayambashic, Y Wei, "Microporous silica-supported cation exchanger with superior dimensional stability and outstanding exchange kinetics, and its application in element removal and enrichment," *React. Funct. Polym*, **142** 87-95 (2017). doi: 10.1016/j.reactfunctpolym.2019.06.007.
7) X. Jiang, H. Zhang, M. Yue, S. Zhang, Y. Li, and W. Xu, "Synthesis of organic hybrid super-microporous silicas as an adsorbent for dyes removal from water," *Microporous Mesoporous Mater.*, **288** 109598 (2019). doi: 10.1016/j.micromeso.2019.109598
8) M. Sultan, I.I. El-Sharkawl, T. Miyazaki, B.B. Saha, and S. Koyama, "Experimental study on carbon based adsorbents for greenhouse dehumidification,"

Evergreen, **1** (*2*) 5–11 (2014). doi:10.5109/1495157.
9) D.M. Abouelella, S.E.K. Fateen, and M.M.K. Fouad, "Multiscale modeling study of the adsorption of co2 using different capture materials," *Evergreen*, **5** (*1*) 43–51 (2018). doi:10.5109/1929729.
10) P. Pal, A.K. Nayak, and R. Dev, "A modified double slope basin type solar distiller: experimental and enviro-economic study," *Evergreen*, **5** (*1*) 52–61 (2018). doi:10.5109/1929730.
11) S. Silviana, D.D. Anggoro, C.A. Salsabila, and K. Aprilio, "Utilization of geothermal waste as a silica adsorbent for biodiesel purification," *Korean J. Chem. Eng.*, **38** (*10*) 2091–2105 (2021). doi:10.1007/s11814-021-0827-z.
12) M.H. Mahmood, M. Sultan, and T. Miyazaki, "Study on water-vapor adsorption onto polymer and carbon based adsorbents for air-conditioning applications," *Evergreen*, **6** (*3*) 215–224 (2019). doi:10.5109/2349297.
13) R. Karimi-Chayjani, N. Daneshvar, M.S.N. Langarudi, F. Shirini, and H. Tajik, "Silica-coated magnetic nanoparticles containing bis dicationic bridge for the synthesis of 1, 2, 4-triazolo pyrimidine/quinazolinone derivatives," *J. Mol. Struct.*, **1199** 126891 (2020). doi: 10.1016/j.molstruc.2019.126891
14) S. Hanif, M. Sultan, T. Miyazaki, and S. Koyama, "Steady-state investigation of desiccant drying system for agricultural applications," *Evergreen*, **5** (*1*) 33–42 (2018). doi:10.5109/1929728.
15) M.H. Mahmood, M. Sultan, T. Miyazaki, and S. Koyama, "Desiccant air-conditioning system for storage of fruits and vegetables: pakistan preview," *Evergreen*, **3** (*1*) 12–17 (2016). doi:10.5109/1657381.
16) S. He, D. Huang, H. Bi, Z. Li, H. Yang, and X. Cheng, "Synthesis and characterization of silica aerogels dried under ambient pressure bed on water glass," *J. Non. Cryst. Solids*, **410** 58–64 (2015). doi:10.1016/j.jnoncrysol.2014.12.011.
17) S. Silviana, A. Darmawan, F. Dalanta, A. Subagio, F. Hermawan, and H.M. Santoso, "Superhydrophobic coating derived from geothermal silica to enhance material durability of bamboo using hexadimethylsilazane (hmds) and trimethylchlorosilane (tmcs)," *Materials (Basel).*, **14** (*3*) 1–20 (2021). doi:10.3390/ma14030530.
18) M. Sivasakthi, R. Jeyalakshmi, N.P. Rajamane, "Effect of change in the silica modulus of sodium silicate solution on the microstructure of fly ash geopolymers," *FJ. Build. Eng.*, **44** 102939 (2021). doi: 10.1016/j.jobe.2021.102939.
19) O.O. Amu, and A.A. Adetuberu, "Characteristics of bamboo leaf ash stabilization on lateritic soil in highway construction," *Int. J. Eng. Technol.*, **2** (*4*) 212–219 (2010).
20) S. Affandi, H. Setyawan, S. Winardi, A. Purwanto, and R. Balgis, "A facile method for production of high-purity silica xerogels from bagasse ash," *Adv. Powder Technol.*, **20** (*5*) 468–472 (2009). doi:10.1016/j.apt.2009.03.008.
21) S. Silviana, E.A.P.P. Sagala, S.E. Sari, and C.T.M. Siagian, "Preparation of mesoporous silica derived from geothermal silica as precursor with a surfactant of cethyltrimethylammonium bromide," *AIP Conf. Proc.*, **2202** (*2019*) (2019). doi:10.1063/1.5141683.
22) S. Silviana, G.J. Sanyoto, and A. Darmawan, "Preparation of geothermal silica glass coating film through multi-factor optimization," *J. Teknol.*, **83** (*4*) 41–49 (2021). doi:10.11113/jurnalteknologi.v83.16377.
23) A. Purnomo, F. Dalanta, A.D. Oktaviani, and S. Silviana, "Superhydrophobic coatings and self-cleaning through the use of geothermal scaling silica in improvement of material resistance," *AIP Conf. Proc.*, **2026** (2018). doi:10.1063/1.5065037.
24) S. Silviana, G.J. Sanyoto, A. Darmawan, and H. Sutanto, "Geothermal silica waste as sustainable amorphous silica source for the synthesis of silica xerogels," *Rasayan J. Chem.*, **13** (*3*) 1692–1700 (2020). doi:10.31788/RJC.2020.1335701.
25) B. Prasetyo, Suyanto, M.A.M. Oktaufik, and S. Himawan, "Design, construction and preliminary test operation of bppt-3mw condensing turbine geothermal power plant," *Evergreen*, **6** (*2*) 162–167 (2019). doi:10.5109/2321012.
26) Y. Gunawan, N. Putra, E. Kusrini, I.I. Hakim, and M.D.H. Setiawan, "Study of heat pipe utilizing low-temperature geothermal energy and zeolite-a for tea leaves withering process," *Evergreen*, **7** (*2*) 221–227 (2020). doi:10.5109/4055223.
27) D. Mutebi, A.A. Nur, A.D. Haryanto, and J. Wiwid, "Variation of rock electrical resistivity in andesitic-trachytic volcanic geothermal areas. a case study of lili-sepporaki, sulawesi island-indonesia," *Evergreen*, **7** (*3*) 314–322 (2020). doi:10.5109/4068609.
28) H. Xu, W. pin Huang, K. feng Ren, and Y. min Tang, "Spraying layer-by-layer assembly of tannin-fe3+ and polyethyleneimine for antibacterial coating," *Colloids Interface Sci. Commun.*, **42** (*March*) 100422 (2021). doi:10.1016/j.colcom.2021.100422.
29) Q.H. Tran, V.Q. Nguyen, and A.T. Le, "Silver nanoparticles: synthesis, properties, toxicology, applications and perspectives," *Adv. Nat. Sci. Nanosci. Nanotechnol.*, **4** (*3*) (2013). doi:10.1088/2043-6262/4/3/033001.
30) J. Pilipavicius, A. Chodosovskaja, A. Beganskiene, and A. Kareiva, "Silver nanoprisms self-assembly on differently functionalized silica surface," *IOP Conf. Ser. Mater. Sci. Eng.*, **77** (*1*) (2015). doi:10.1088/1757-899X/77/1/012006.
31) S. Silviana, I.N.H. Rambe, H. Sudrajat, and M.A. Zidan, "Statistical approaching of sol-gel process in preparation of silica aerogel derived from geothermal silica by several acids," *AIP Conf. Proc.*, **2202**

(*December 2019*) (2019). doi:10.1063/1.5141682.
32) F. Meyori, R. Elvia, and I.N. Candra, "Kopresipitasi dari pasir pantai panjang bengkulu," *J. Pendidik. Dan Ilmu Kim.*, **2** (*1*) 46–51 (2018).
33) J. Pilipavicius, R. Kaleinikaite, M. Pucetaite, M. Velicka, A. Kareiva, and A. Beganskiene, "Controllable formation of high density sers-active silver nanoprism layers on hybrid silica-aptes coatings," *Appl. Surf. Sci.*, **377** 134–140 (2016). doi:10.1016/j.apsusc.2016.03.169.
34) S.W. Hwang, T.Y. Kim, and S.H. Hyun, "Optimization of instantaneous solvent exchange/surface modification process for ambient synthesis of monolithic silica aerogels," *J. Colloid Interface Sci.*, **322** (*1*) 224–230 (2008). doi:10.1016/j.jcis.2008.02.060.
35) S.H.S. Md. Fadzullah, M.M. Nasaruddin, Z. Mustafa, W.A.W.A. Rahman, G. Omar, M.A. Salim, and M.R. Mansor, "The effect of chemical surface treatment on mechanical performance of electrically conductive adhesives," *Evergreen*, **7** (*3*) 444–451 (2020).
36) Y. Soga, H. Imanaka, K. Imamura, and N. Ishida, "Effect of surface hydrophobicity on short-range hydrophobic attraction between silanated silica surfaces," *Adv. Powder Technol.*, **26** (*6*) 1729–1733 (2015). doi:10.1016/j.apt.2015.10.017.
37) A. Riveiro, A.L.B. Maçon, J. del Val, R. Comesaña, and J. Pou, "Laser surface texturing of polymers for biomedical applications," *Front. Phys.*, **5** (*FEB*) (2018). doi:10.3389/fphy.2018.00016.
38) K. Wei, H. Zeng, and Y. Zhao, "Substrate material affects wettability of surfaces coated and sintered with silica nanoparticles," *Appl. Surf. Sci.*, **273** 32–38 (2013). doi:10.1016/j.apsusc.2013.01.077.
39) N.K. Sethy, Z. Arif, P.K. Mishra, and P. Kumar, "Synthesis of sio2 nanoparticle from bamboo leaf and its incorporation in pdms membrane to enhance its separation properties," *J. Polym. Eng.*, **39** (*7*) 679–687 (2019). doi: 10.1515/polyeng-2019-0120
40) I.H. Dwirekso, M. Ibadurrohman, and Slamet, "Synthesis of tio2-sio2-cuo nanocomposite material and its activities for self-cleaning," *Evergreen*, **7** (*2*) 285–291 (2020). doi:10.5109/4055234.
41) B. Poerwadi, C.W. Kartikowati, R. Oktavian, and O. Novaresa, "Manufacture of a hydrophobic silica nanoparticle composite membrane for oil-water emulsion separation," *Int. J. Technol.*, **11** (*2*) 364–373 (2020). doi:10.14716/ijtech.v11i2.3279.
42) H. Kim, and J.-Y. Kwon, "Enzyme immobilization on metal oxide semiconductors exploiting amine functionalized layer," *RSC Adv.*, **7** (*32*) 19656–19661 (2017). doi: 10.1039/C7RA01615H
43) M.A. Pratama, G. Ramahdita, and A.H. Yuwono, "The effect of silver nitrate addition on antibacterial properties of bone scaffold chitosan-hydroxyapatite," *AIP Conf. Proc.*, **2193** (*December*) (2019). doi:10.1063/1.5139334.
44) M. Ydollahi, H. Ahari, and A.A. Anvar, "Antibacterial activity of silver-nanoparticles against staphylococcus aureus," (*June*) (2016). doi:10.5897/AJMR2016.7908.
45) J. Wang, Y. Chen, Y. Chen, and J. Li, "Fabrication and characterization of superhydrophilic and antibacterial surfaces by silver nanoparticle self-assembly," *Colloid Polym. Sci.*, **295** (*11*) 2191–2196 (2017). doi:10.1007/s00396-017-4179-5.
46) P.P.D.K. Wulan, J.A. Ningtyas, and M. Hasanah, "The effect of nickel coating on stainless steel 316 on growth of carbon nanotube from polypropylene waste," *Evergreen*, **6** (*1*) 98–102 (2019). doi:10.5109/2328411.